SEARCH FOR EXOTIC MESONS: RECENT RESULTS FROM BNL EXPERIMENT E852

P. EUGENIO

University of Massachusetts–Dartmouth for the E852 Collaboration (Brookhaven, Indiana, IHEP Protvino, Massachusetts–Dartmouth, Moscow State, Northwestern, Notre Dame, Rensselaer)

Preliminary analyses are shown for charged and neutral final meson states produced in $\pi^- p$ interactions. A partial wave analysis has been carried out to search for possible exotic meson states. Preliminary results exhibit relative phase motions which are consistent with resonant exotic states.

1 Introduction

At short distances the strong interaction is well described by methods of perturbative QCD. But at large distances, the regime of quark confinement, the tools of perturbative QCD break down because gluons carry color charge and so can interact with other gluons. [1] Corrections for the gluon self–coupling lead to a non-perturbative QCD.

Studies of meson spectra via strong decays of hadrons provide insight regarding QCD at the confinement scale. These studies have lead to phenomenological models for QCD such as the constituent quark model. In the constituent quark model, mesons are made of a quark and an antiquark ($q\bar{q}$) bound together. The constituent quark model works surprisingly well— it leads to the familiar multiplet structure of mesons. However, QCD demands a much richer spectrum of meson states. These extra states, known as hybrids ($q\bar{q}g$) and glueballs (gg) are attributed to an additional gluonic degree of freedom.

Another model which approximates QCD is the flux-tube model. In the flux-tube model, the gluon's strong self-interactions are represented by quarks being held together by a color line of flux. [2] The chromoelectric flux can be excited just like plucking a string. The ground states of the flux-tube are identified as $q\bar{q}$ mesons, whereas excited states correspond to hybrid mesons. Hybrids decaying to two ground state mesons (two S-wave state $q\bar{q}$ mesons) such as $\pi\pi$, are suppressed in the flux-tube model. The favored decays are to P-wave and S-wave final state meson pairs such as $b_1(1235)\pi$ and $f_1(1285)\pi$. But a recent extension of the flux-tube model suggests that hybrids decaying to two S-wave $q\bar{q}$ mesons are not completely negligible. Moreover, due to kinematical suppression of the preferred hybrid decays (S-wave and P-wave meson pairs), the flux-tube model predicts that some hybrids should have dominant decays to two S-wave $q\bar{q}$ mesons such as $\rho\pi$ and $\omega\eta$.[3]

The search for mesons beyond the constituent quark model is the scope of this discussion. Recent experiments have focused on searching for the forbidden $q\bar{q}$ states [4,5,6,7]; in particular, Brookhaven National Laboratory Experiment E852, *A Search for Mesons with Unusual Quantum Numbers*, of which recent results are presented here.

In general, there are two methods to search for these hybrid states:

1. Look for an excess of meson states which cannot be explained by the quark model.

2. Look for meson states which are forbidden by the quark model.

The first method is more troublesome since hybrid states could be indistinguishable from $q\bar{q}$ states, and also hybrids could mix with $q\bar{q}$ mesons. A more concrete approach is to search for the forbidden quark model states—the exotic states. Since $q\bar{q}$ mesons are either in a spin singlet or spin triplet state, meson with quantum numbers $J^{PC} = 0^{--}, 1^{-+}, 2^{+-}, 3^{-+}, +...$ are forbidden by the quark model.[a] These quantum numbers are referred to as exotic quantum numbers. An observation of an exotic state is direct evidence for a non-$q\bar{q}$ meson.

2 E852 Detectors

Experiment E852 being carried out at Brookhaven National Laboratory is an experiment in meson spectroscopy with a focus on studying both neutral and charged final states of $\pi^- p$ collisions in a search for meson states beyond the quark model. Brookhaven's Alternating Gradient Synchrotron (AGS) delivers an 18 GeV/c π^- beam to the Multi-Particle Spectrometer facility (MPS). The MPS facility, which was augmented with additional detectors designed specifically for E852, consists of 3 integral regions: target, charged tracking, and downstream regions (See Figure 1).

A π^- beam is transported to a 30 cm long liquid hydrogen target which is located in the center of a large aperture 1 tesla dipole magnet. Surrounding the target is a cylindrical drift chamber (TCYL) consisting of four cylindrical chambers with axial wires.[8] The chamber utilizes charge-division readout. TCYL measures the recoiling proton track and provides this information for both event triggering and off-line analysis. Surrounding TCYL is a 198 block

[a] J^{PC} quantum numbers: J= total angular momentum, P= parity, C= charge conjugation.

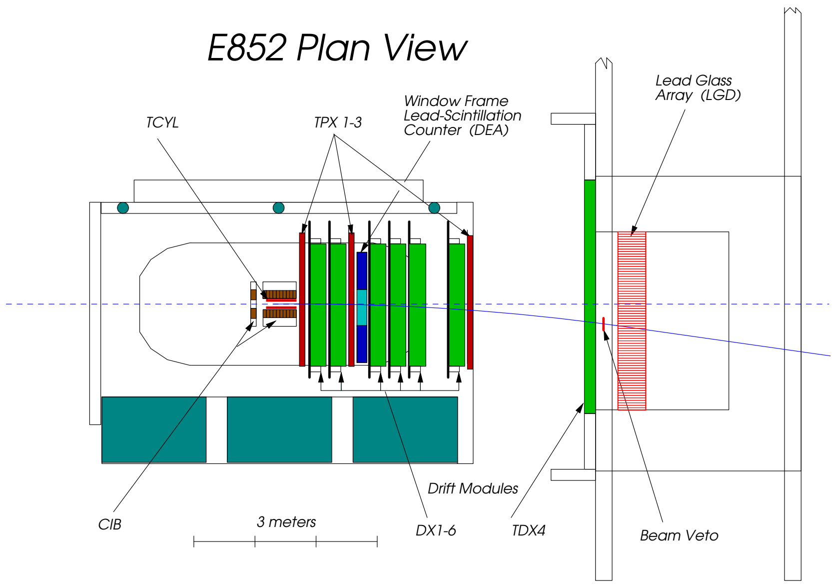

Figure 1: The plan view of E852 at the MPS facility

CsI barrel veto detector (CIB).[9] CIB is used off-line to veto events where soft photons miss the down stream neutral detectors.

Located within the downstream end of the MPS magnet is the charged tracking region. For fast triggering, there are three porportional wire chambers (TPX1–3) that provide information about the charged track multiplicities. Precision tracking is performed with the use of six seven-layer drift chambers DX1-6.[10] In addition to the tracking chambers, there is a window-frame lead/scintillator sandwich veto detector (DEA) and a two unit scintillator veto (CPVB and CPVC). CPVC masks the DEA and together the counters are used off-line to veto events where gammas miss the downstream detection region and the CIB veto. Also, CPVB which covers the window hole in DEA, and CPVC are used as trigger elements for the all-neutral final states.

The bulk of the neutral detection is performed in the downstream region. The main component is a 3045 element lead–glass calorimeter (LGD) for detecting and measuring the energy of forward going gammas.[11] In conjunction with a hardware processor, the LGD is used in the trigger to enrich data that requires a set value of neutral mass (e.g. an η or π^0) in the final state. In addition to the LGD, there is a large drift chamber (TDX4) which is located in front of the LGD. TDX4's main task is to tag the charged particles that interact in the LGD which otherwise could masquerade as gammas.

3 E852 Results

In this paper, preliminary analyses are shown for charged and neutral final meson states produced at 18 GeV/c beam momentum in the reactions:

1. $\pi^- p \rightarrow X^0 n$
   where $X^0 \rightarrow \omega\pi^0$
2. $\pi^- p \rightarrow X^- p$
   where $X^- \rightarrow \pi^+\pi^-\pi^-$
3. $\pi^- p \rightarrow X^- p$
   where $X^- \rightarrow \eta\pi^-$

The data for these analyses were collected during the summer of 1994. The MPS facility's trigger electronics and data acquisition system, which were upgraded for E852, permitted data taking rates of up to 700 events per AGS beam spill ($2\text{x}10^6 particles$) resulting in a total of 250 million physics triggers of various types. An additional 750 million triggers were acquired during the 1995 data run which is currently being processed.

3.1 $\omega\pi^0$

A study of the $\omega\pi^0$ system has been carried out to search for possible exotic meson states. An attractive feature of this channel is that both the π^0 and the ω are relatively narrow resonances. Prominant ω and η resonances are seen in the accepted 3π effective mass spectrum, see Figure 2a. The $\omega\pi^0$ final state contains two well-known mesons, the $b_1(1235)$ and the $\rho_3(1690)$. $\omega\pi^0$ is also of importance in the study of exotics in the $b_1\pi$ final state— a flux–tube favored decay for exotics. In order to perform a detailed partial wave analysis of $b_1\pi$, all $\omega\pi$ isobars in the b_1 region need to be taken into account. Thus, a full understanding of $\omega\pi$ near the b_1 is necessary.

The $b_1(1235)$ and $\rho_3(1690)$ are clearly seen in the accepted $\omega\pi$ effective mass spectrum of Figure 2b. An interesting feature is the $\rho_3(1690)$ dependence on the transverse momentum ($|t|$). Figure 3 shows that $\rho_3(1690)$ is produced strongly at low $|t|$. The low $|t|$ dependence suggest that the production mechanism is one–pion exchange.

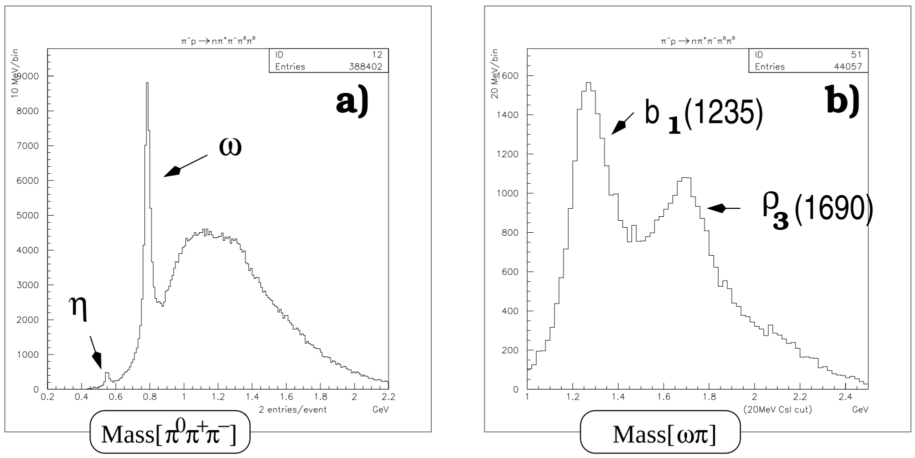

Figure 2: The effective mass spectra for the $\omega\pi$ final state. a) The 3 π effective mass (2 entries per event). b) The 4 π effective mass with the requirement that a 3 π effective mass be an ω.

Figures 4 and 5 display the results of the partial wave analysis. As expected, there are clear signals for b_1 in the 1^{+-} wave and ρ_3 in the 3^{--} wave. It should be noted that the two exotic waves, 0^{--} and 2^{+-}, do not show any well-founded indication of resonant structure.

As noted earlier, the ρ_3 is expected to be produced by one–pion exchange. Figure 6 depicts the ρ_3 production plane. Since both the beam and the exchange pion are spinless, the total spin of the ρ_3 is due to orbital angular momentum of the production pions. For one-pion exchange to be valid, the ρ_3 must be produced with zero spin component along the beam because the orbital angular momentum must lie normal to the production plane.

The partial wave amplitudes are parameterized according to the conviention developed by S.U. Chung [13]. In this formalism, the basis states used are the reflectivity basis states. For the reflectivity basis, the spin component along the axis of quantization[b], M, is replaced by $|M|$ and the reflectivity (ϵ). The reflectivity is defined as the negative of the eigenvalue of the reflection operator, which also coincides with the naturality of the exchanged meson: $\epsilon = P(-1)^J$ [14]. Since a π has $J^P = 0^-$, a one-pion exchange should have $\epsilon = -1$. A more detailed description of the PWA formalism is given in these proceedings [12].

For this analysis, the 3 amplitudes which make up the 3^{--} wave are shown

[b] The beam defines the axis of quantization

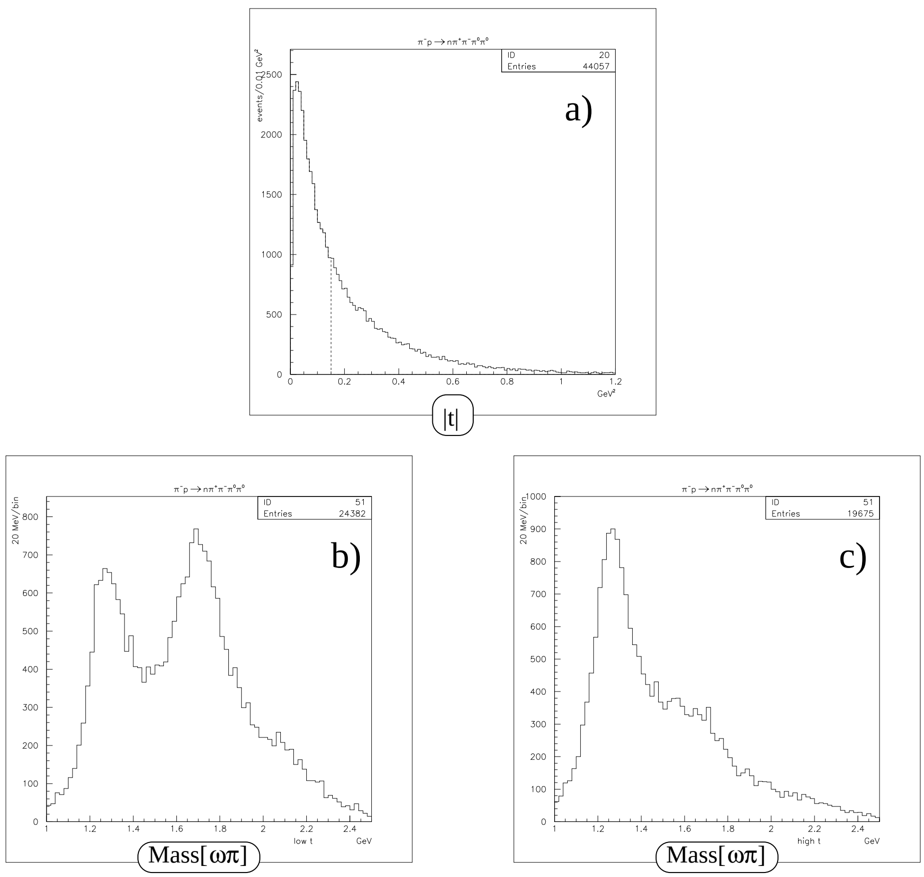

Figure 3: The $\omega\pi$ spectrum dependence on the transverse momentum. a) transverse momentum $(\mathrm{GeV/c^2})^2$ b) $\omega\pi$ spectrum for $0 < |t| < 0.15$ c) $\omega\pi$ spectrum for $0.15 < |t| < 1.2$

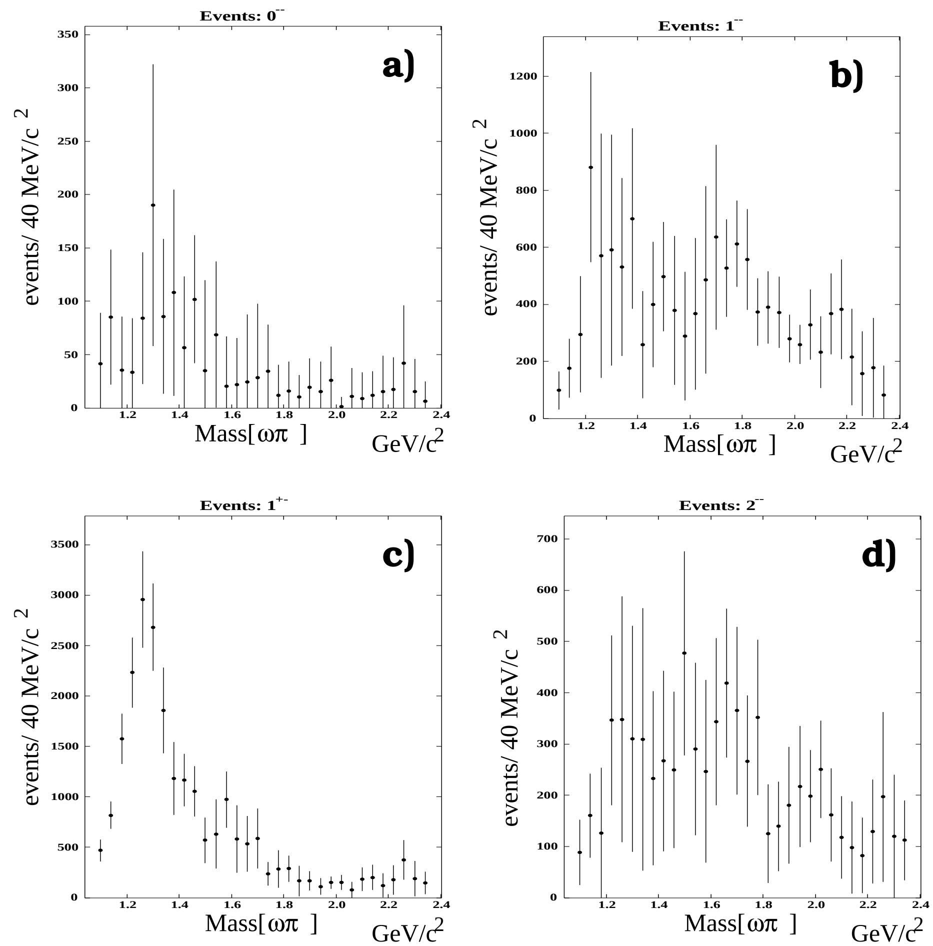

Figure 4: Partial wave intensities for $\omega\pi$. a) $J^{PC} = 0^{--}$, b) $J^{PC} = 1^{--}$, c) $J^{PC} = 1^{+-}$, d) $J^{PC} = 2^{--}$

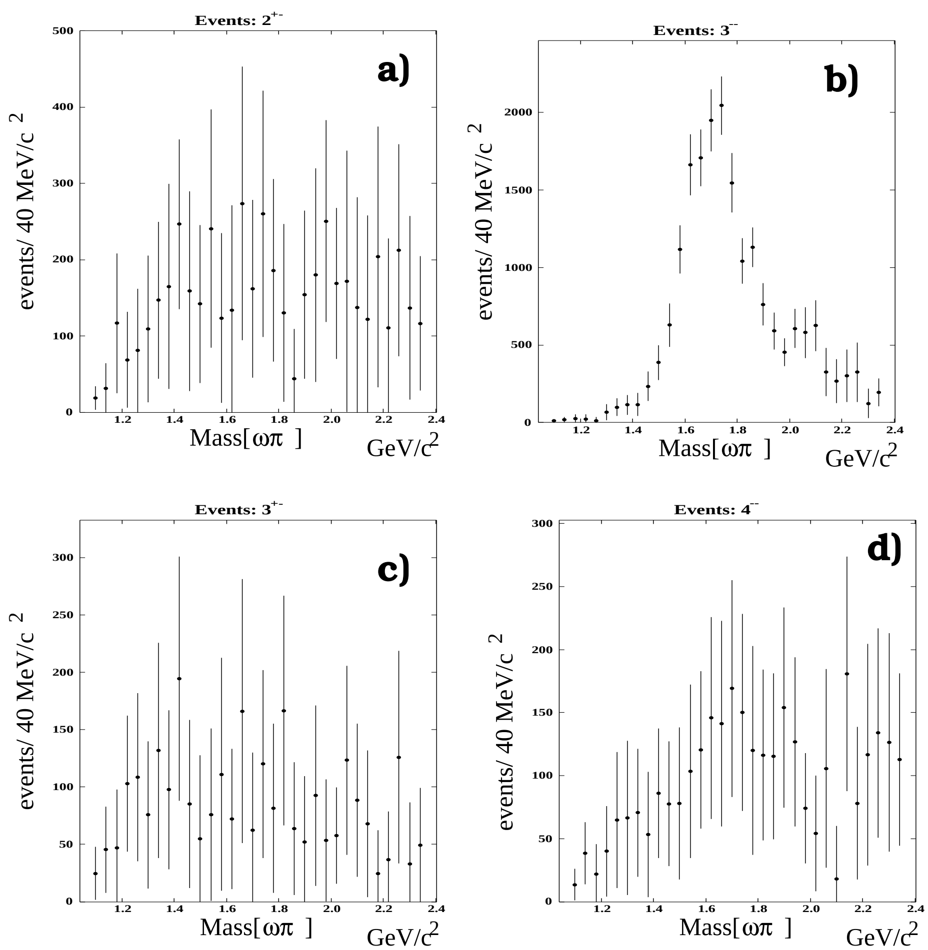

Figure 5: Partial wave intensities for $\omega\pi$. a) $J^{PC} = 2^{+-}$, b) $J^{PC} = 3^{--}$, c) $J^{PC} = 3^{+-}$, d) $J^{PC} = 4^{--}$

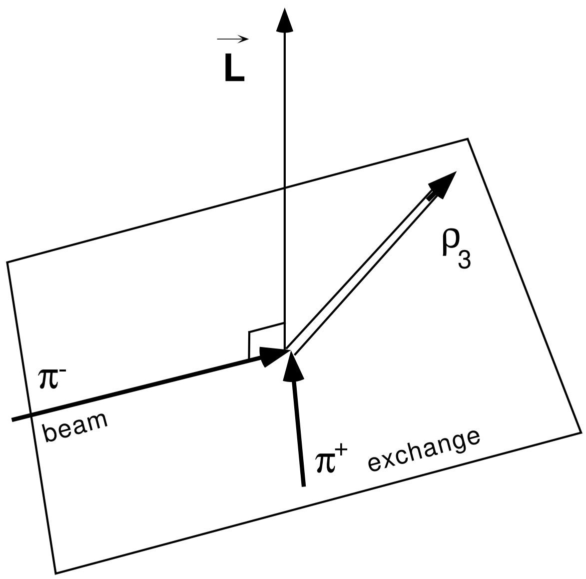

Figure 6: The ρ_3 production plane.

in Figure 7. The $\rho_3(1690)$ is produced dominantly in the $M^\epsilon = 0^-$ state as expected by one-pion exchange.

3.2 $\pi^+\pi^-\pi^-$

The $\pi^+\pi^-\pi^-$ system is of special interest because several experiments have reported evidence of a $J^{PC} = 1^{-+}$ produced only in natural parity exchange. It is likely that this exchange is dominated by ρ exchange.[15] This leads to the expectation that hybrids might significantly couple to $\rho\pi$. Figure 8a shows the accepted $\pi^+\pi^-\pi^-$ effective mass spectrum. The $a_2(1320)$ and $\pi_2(1670)$ are clearly seen in the spectrum. In addition, a broad $a_1(1160)$ shoulder is also noticeable. The ρ and $f_2(1270)$ are clearly seen to dominate the $\pi^+\pi^-$ effective mass spectrum as shown in Figure 8b.

The results of the partial wave analysis are shown in Figure 9 and Figure 10. In $J^{PC} = 0^{-+}$, the broad $\pi(1300)$ is seen. Also, $\pi(1800)$, previously reported by VES is seen.[6] The rising $(0^{-+} - 2^{-+})$ phase difference in the 1800 MeV/c^2 mass region suggests that the $\pi(1800)$ is resonant. $a_1(1160)$, $a_2(1320)$ and $\pi_2(1670)$ are clearly seen in the 1^{++}, 2^{++}, and the 2^{-+} waves respectively. The exotic $J^{PC} = 1^{-+}$ wave has two significant peaks, one

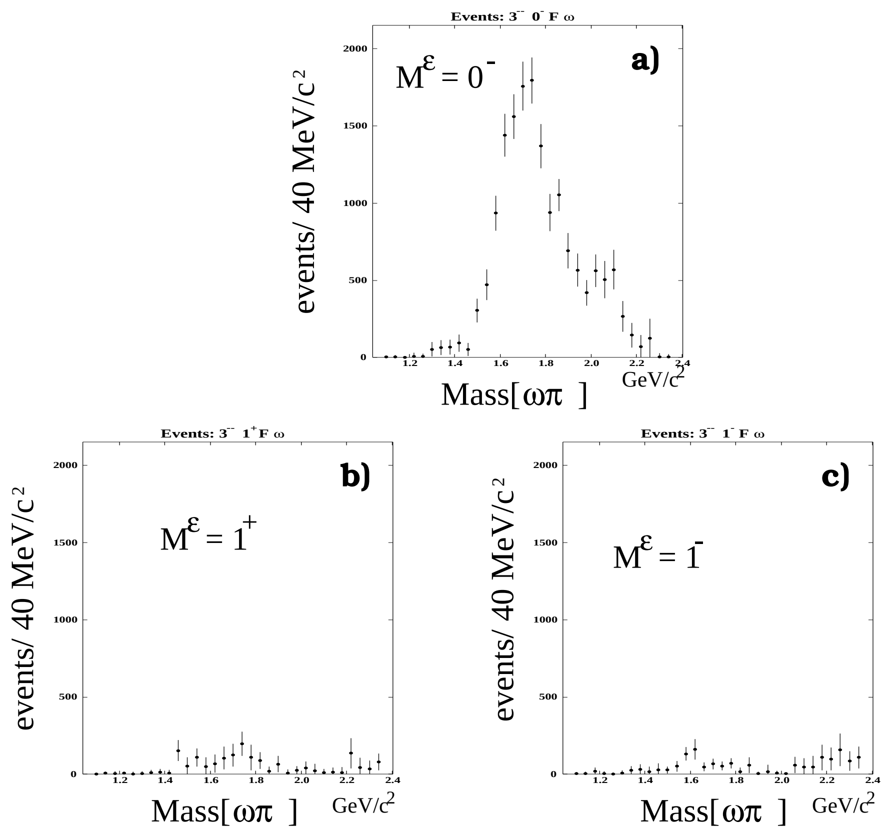

Figure 7: Partial wave amplitude intensities for the 3^{--} wave. a) $J^{PC}M^{\epsilon} = 3^{--}0^{-}$, b) $J^{PC}M^{\epsilon} = 3^{--}1^{+}$, c) $J^{PC}M^{\epsilon} = 3^{--}1^{-}$

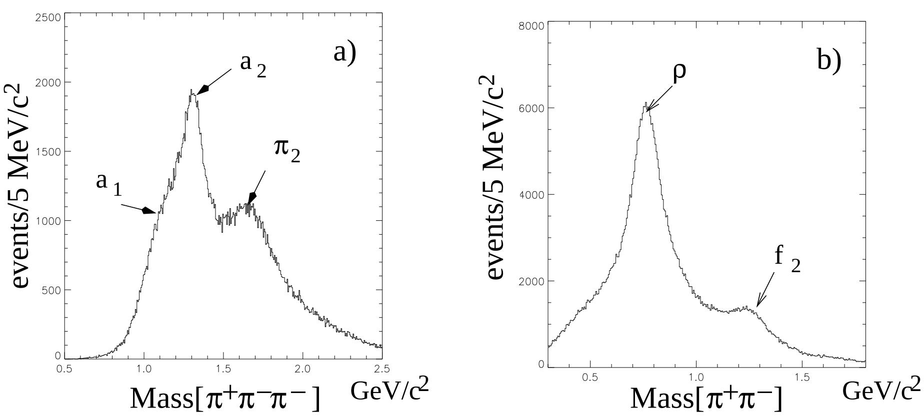

Figure 8: Effective mass spectrum for the 3π final state. a)$\pi^+\pi^-\pi^-$ b) $\pi^+\pi^-$.

near 1200-1300 MeV/c^2 and the other at 1600 MeV/c^2. The 1^{-+} peak at 1600 MeV/c^2 exhibits relative phase motion which is consistent with resonant structure. Currently in progress is a detailed study of the phase motions and possible leakage from non–exotic waves into the 1^{-+} wave due to the finite apparatus acceptance.

3.3 $\eta\pi^-$

The $\eta\pi^-$ system is also of special interest because all odd partial waves are necessarily exotic. Thus, observation of a P–wave resonance is strong evidence of a $J^{PC} = 1^{-+}$ exotic meson. Previous experimental results suggest the presence of a significant P–wave in this system. [5] Shown in Figure 11 is the accepted $\eta\pi^-$ effective mass spectrum. These events are clearly dominated by $a_2(1320)$ production. Shown in Figure 12 is the acceptance–corrected (η forward $-$ η backward) decay asymmetry versus the $\eta\pi^-$ effective mass. There is a strong asymmetry which can only arise from the interference of even and odd partial waves. This asymmetry is an indication of the presence of an exotic wave.

Results for the amplitude analysis are displayed in Figure 13. Shown are the 2^{++} intensity, 1^{-+} intensity, and the $(1^{-+} - 2^{++})$ phase diference. The other waves are small. The 2^{++} intensity is dominated by the $a_2(1320)$. The 1^{-+} intensity shows a significant peak at 1300 MeV/c^2, and in addition, the relative phase motion is consistent with both the non–exotic 2^{++} and the

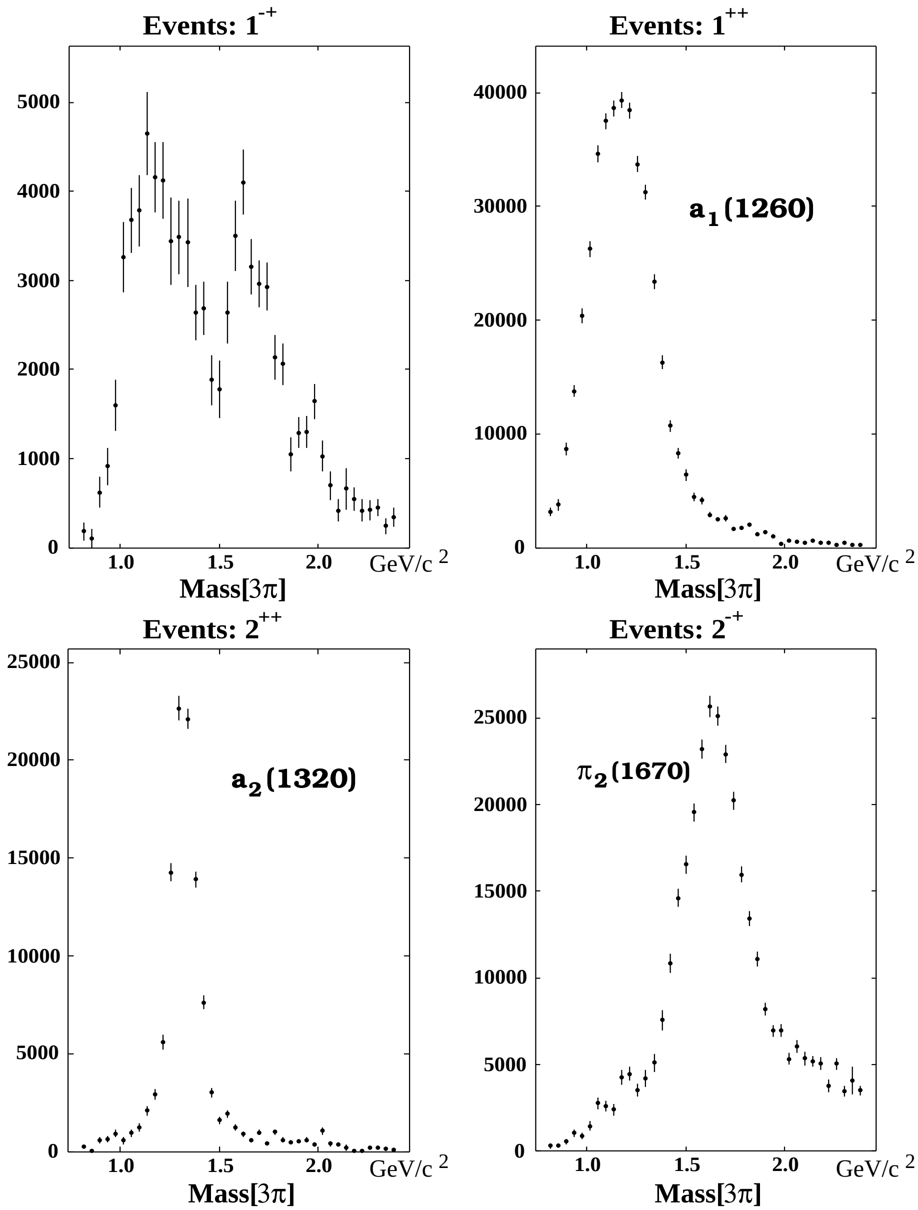

Figure 9: Partial wave intensities for $\pi^+\pi^-\pi^-$ (events/ 40 MeV/c^2).

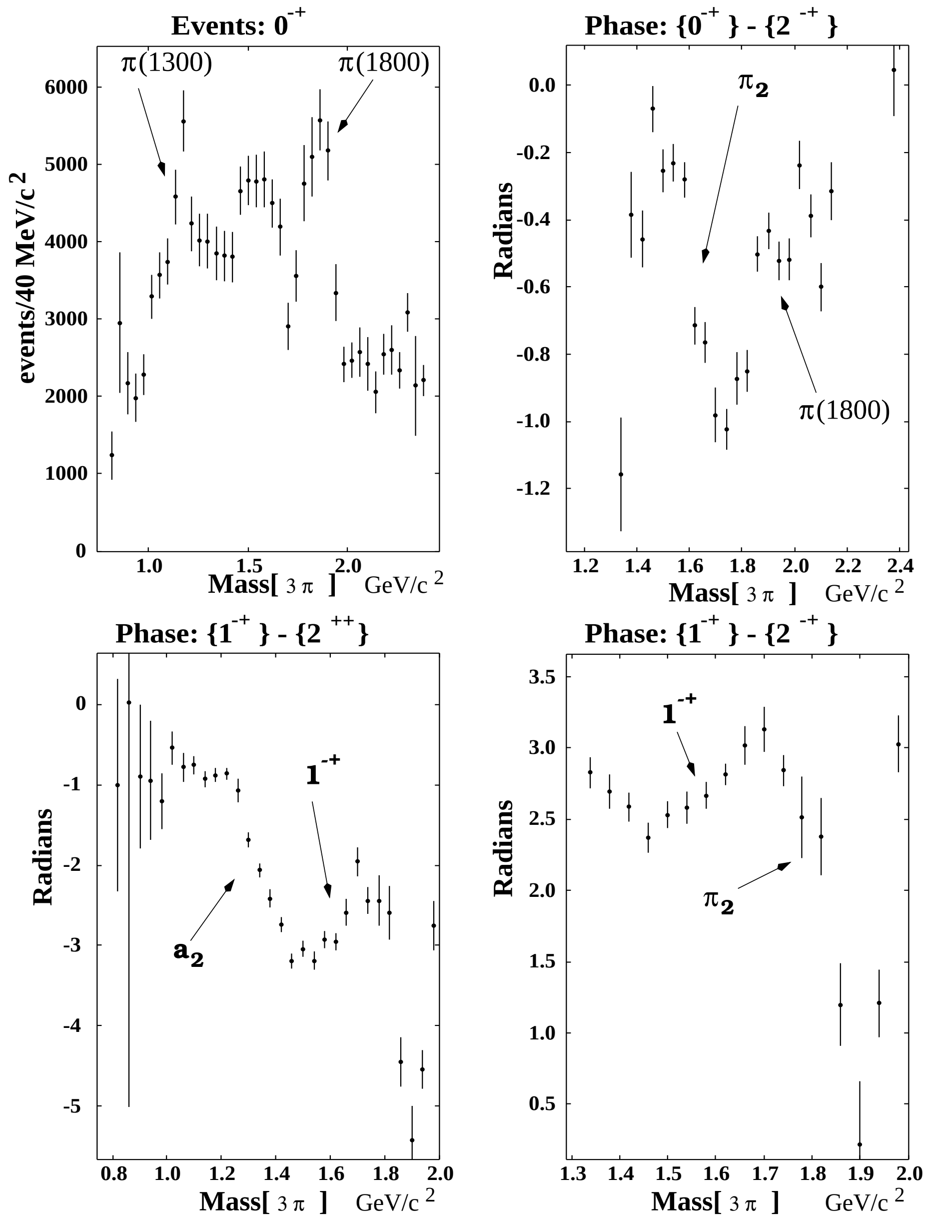

Figure 10: PWA phase results for $\pi^+\pi^-\pi^-$.

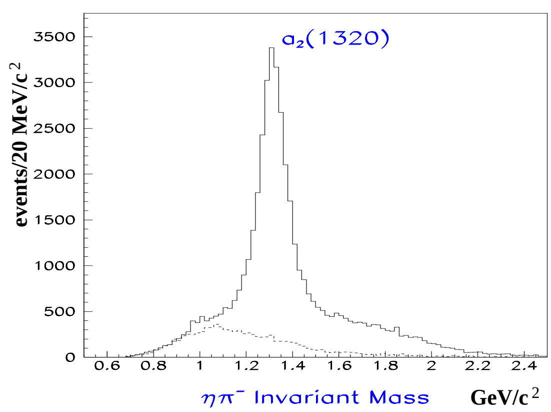

Figure 11: Effective mass spectrum for $\eta\pi^-$. Dashed histogram is the background estimated from the eta side bands.

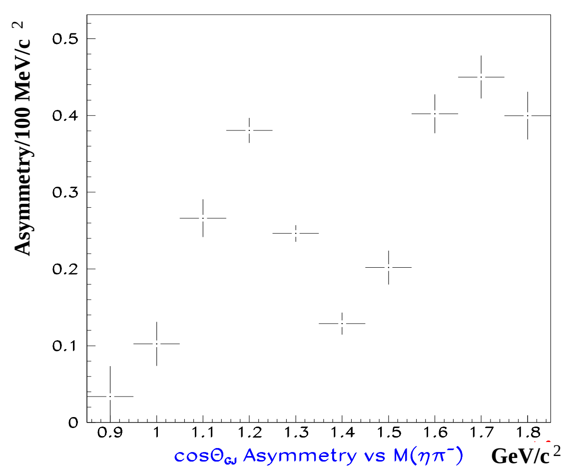

Figure 12: $\eta\pi^-$ decay asymmetry (forward − backwards)/(forward + backwards). $-0.8 < cos\Theta_{GJ} < 0.8$

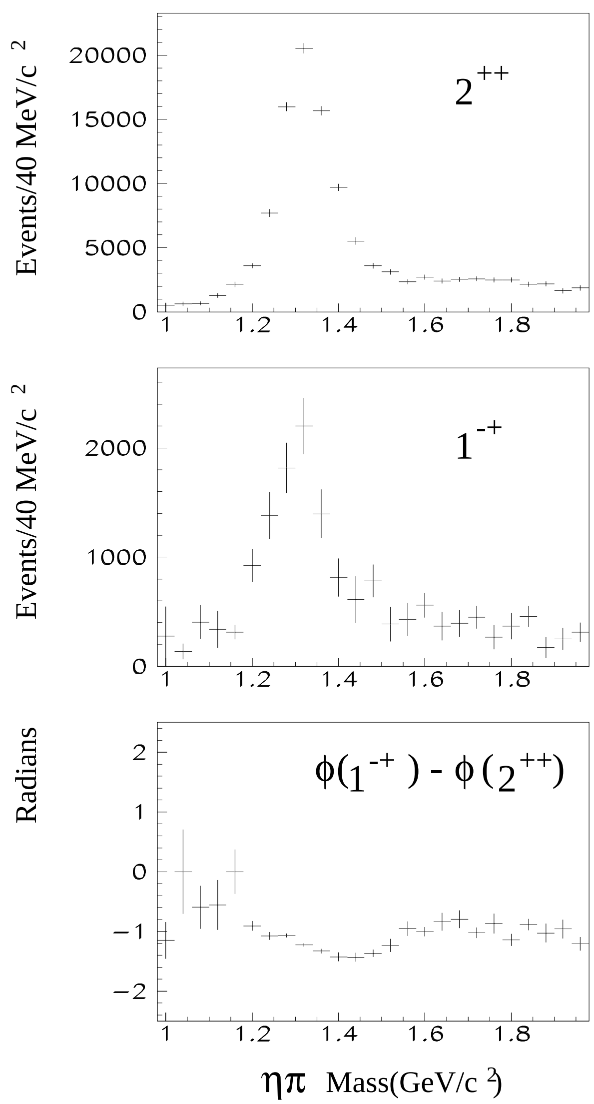

Figure 13: $\eta\pi^-$ 2^{++} and 1^{-+} intensities and the $(1^{-+} - 2^{++})$ phase difference.

exotic 1^{-+} resonating. A detailed analysis of the phase motion is currently in progress.

Acknowledgments

This work was supported in part by NSF grants PHY–9001389 and PHY–9302063 at the University of Massachusetts–Dartmouth, PHY–9120649 at the University of Notre Dame, and PHY–9507412 at Rensselear Polytechnic Institute; and by DOE grants DE–AC02–76CH00016 at Brookhaven National Laboratory, DE–FG02–91er40661 at Indiana University, DE–FG02–91ER40623 at the University of Notre Dame, and DE–FG02–87–ER40344 at Northwestern University.

References

1. M.R. Pennington, Durham *Proceedings of the VIth International Conference on Hadron Spectroscopy*, Summary:Part 1 (1996)
2. N. Isgur and J. Paton , *Phys. Rev.* D **31**, 2910 (1985)
3. F. Close and P. Page, *Nucl. Phys.* B **443**, 233 (1995)
4. D. Alde *et al*, *Phys. Lett.* **B205**, 397 (1988)
5. H. Aoyagi *et al*, *Nuovo Cimento* **107**, 1925 (1994)
6. Yu.P. Gouz *et al*, VES *Proceedings of the XXVI International Conference on High Energy Physics*, 572 ()
7. J.H. Lee *et al*, *Phys. Lett.* B **B323**, 227 (1994)
8. Z. Bar–Yam *et al*, *Nucl. Instrum. Methods* A , (1996) submitted.
9. T. Adams *et al*, *Nucl. Instrum. Methods* A **368**, 617 (1996)
10. S. Eiseman *et al*, *Nucl. Instrum. Methods* **217**, 140 (1983)
11. B.B. Brabson *et al*, *Nucl. Instrum. Methods* A , (1996) submitted.
12. J.P. Cummings, these proceedings.
13. S.U. Chung, Brookhaven **BNL-QGS-93-05**, preprint (1993)
14. J.P. Cummings, Rice University *A Study of the $K^+\bar{K}^0\pi^-$ System Produced in the Reaction $\pi^- p \to K^+\bar{K}^0\pi^- n$ at 18 GeV/c* , thesis (1995)
15. D. Weygand *et al*, BNL–E852 *Proceedings of the VIth International Conference on Hadron Spectroscopy*, 55 (1996)